

8.0%




Date: 2023-05-12 11:22 UTC

* All sources 27 | Internet sources 25

| | | | | |
|-------------------------------------|------|--|------|---|
| <input checked="" type="checkbox"/> | [1] | www.sciencedirect.com/science/article/pii/S1018364721001282 | 3.1% | 20 matches |
| <input checked="" type="checkbox"/> | [2] | www.ncbi.nlm.nih.gov/pmc/articles/PMC7669941/ | 1.6% | 14 matches |
| <input checked="" type="checkbox"/> | [3] | mutagen-brasil.org.br/_img/_banco_imagens/XIV Congresso da MutaGen_Anais_2019.pdf | 1.1% | 9 matches |
| <input checked="" type="checkbox"/> | [4] | link.springer.com/article/10.1007/s42452-019-0818-4 | 0.9% | 9 matches |
| <input checked="" type="checkbox"/> | [6] | www.mdpi.com/1420-3049/23/7/1637 | 0.6% | 5 matches |
| <input checked="" type="checkbox"/> | [7] | www.mdpi.com/2227-9059/10/10/2442 | 0.6% | 5 matches |
| <input checked="" type="checkbox"/> | [8] | www.sciencedirect.com/science/article/abs/pii/S004313542200848X | 0.5% | 5 matches |
| <input checked="" type="checkbox"/> | [9] | www.ncbi.nlm.nih.gov/pmc/articles/PMC7599573/ | 0.5% | 5 matches |
| <input checked="" type="checkbox"/> | [10] | link.springer.com/article/10.1007/s11634-020-00416-5 | 0.5% | 5 matches |
| <input checked="" type="checkbox"/> | [11] | www.ncbi.nlm.nih.gov/pmc/articles/PMC8223570/ | 0.4% | 4 matches |
| <input checked="" type="checkbox"/> | [12] | journals.lww.com/10.3760/cma.j.issn.0366-6999.20131790 | 0.3% | 2 matches |
| <input checked="" type="checkbox"/> | [13] | link.springer.com/article/10.1007/s42452-019-1295-5 | 0.2% | 4 matches |
| <input checked="" type="checkbox"/> | [14] | www.spandidos-publications.com/10.3892/or.2013.2426/download | 0.2% | 1 matches |
| <input checked="" type="checkbox"/> | [15] | www.mdpi.com/1420-3049/23/8/2046/pdf/1 | 0.2% | 2 matches |
| <input checked="" type="checkbox"/> | [16] | www.ncbi.nlm.nih.gov/pmc/articles/PMC7148648/ | 0.1% | 2 matches |
| <input checked="" type="checkbox"/> | [17] | www.ncbi.nlm.nih.gov/pmc/articles/PMC3541205/ | 0.2% | 1 matches ⊕ 1 documents with identical matches |
| <input checked="" type="checkbox"/> | [19] | www.researchgate.net/figure/RT-PCR-analysis-of-apoptotic-and-anti-apoptotic-marker-genes-in-SGCs-after-transfection_fig9_51411981 | 0.2% | 1 matches |
| <input checked="" type="checkbox"/> | [20] | www.ncbi.nlm.nih.gov/pmc/articles/PMC5300024/ | 0.1% | 2 matches |
| <input checked="" type="checkbox"/> | [21] | www.researchgate.net/figure/Induction-of-a-CD8-CTLs-reactivity-against-breast-cancer-cells-by-vaccination-with-the_fig1_232754522 | 0.2% | 1 matches |
| <input checked="" type="checkbox"/> | [22] | www.ncbi.nlm.nih.gov/pmc/articles/PMC1348016/ | 0.1% | 1 matches |
| <input checked="" type="checkbox"/> | [23] | www.ncbi.nlm.nih.gov/pmc/articles/PMC5370347/ | 0.1% | 1 matches |
| <input checked="" type="checkbox"/> | [24] | www.mdpi.com/1420-3049/27/22/7854/pdf | 0.1% | 1 matches ⊕ 1 documents with identical matches |
| <input checked="" type="checkbox"/> | [26] | www.sciencedirect.com/science/article/abs/pii/S1540748916304436 | 0.0% | 1 matches |
| <input checked="" type="checkbox"/> | [27] | www.mdpi.com/2073-4344/12/10/1231 | 0.1% | 1 matches |
| <input checked="" type="checkbox"/> | [28] | www.ncbi.nlm.nih.gov/pmc/articles/PMC9079820/ | 0.1% | 1 matches |

13 pages, 3874 words

 The document contains a suspicious mixture of alphabets. This could be an attempt of cheating.

PlagLevel: 8.0% selected / 87.7% overall

216 matches from 29 sources, of which 27 are online sources.

Settings

Data policy: *Compare with web sources, Check against my documents*

Sensitivity: *High*

Bibliography: *Bibliography excluded*

Citation detection: *Highlighting only*

Whitelist: --

A comparative cytological study of silver and molybdenum oxide nanostructures against breast cancer cells

Abstract

Cancer is a denying disease, and among a number of cancers types, **breast cancer is a** recurrent in females, which affect word widely. For these reason, the work presented here to show the comparative cytological **responses of breast (MCF-7) cancer cells with** silver and molybdenum oxide nanostructures material. The nanostructures were produced via chemical process and characterized. The crystallinities, their size and phases were determined with XRD, while the structural details were scrutinized **via SEM and TEM** correspondingly. The NRs and NPs were exhibit an estimated diameter of $\sim 50\text{-}60\text{nm}$ and $\sim 15\text{nm}$ separately. A cytotoxicity's studies of MCF-7 cells were sway and reliant to their doses (1 to $100\ \mu\text{L}/\text{mL}$) with $\alpha\text{-MoO}_3\text{NRs}$ and AgNPs established via **MTT and NRU assays**. The ROS were also upsurges slowly **from 105, 124, 132, 148 and 108, 130, 135, 165** with dissimilar concentrations of $\alpha\text{-MoO}_3\text{NRs}$ and AgNPs (**25, 50 and 100 $\mu\text{L}/\text{mL}$ with control** reciprocally. Also gene expression (mRNA extraction) study with apoptotic markers in presence of $\alpha\text{-MoO}_3\text{NRs}$ and AgNPs were up-regulated and shows **apoptosis in cells**. The study provides a possible comparative results related to the cytotoxicity's **in breast (MCF-7) cancer cell** with AgNPs are high as compared to $\alpha\text{-MoO}_3\text{NRs}$ also authenticated via gene expression study.

Keywords: Molybdenum oxide NRs; Silver NPs; **Cytotoxicity, MCF-7 cells**; ROS; RT-PCR.

1.0 Introduction

Among a number of cancers types, the breast cancer is very common to the whole world and affected especially in female candidate (Nardin et al., 2020). As it's known that cancer is a denying disease which affect not only the particular organ but also affect the whole body system (Wahab et al., 2013). An estimated value of the breast cancer, grasp a more than one million women's world wide. A detailed statistical data reveals that cancer increase very widely for instance in 2008, ~421,000 cases were diagnosed for cancers, ~49,500 cases were found in 2009-2010 only in Europe. The breast cancer cases is increases day by day and a new cases (~268,600) were identified in women, also detected in men (~2,670) in 2019 (Nardin et al., 2020). From this divesting disease an average 42,170 women in U.S. to die in 2020 (Breast Cancer Facts & Figures 2019-2020).^[1] A number of techniques have been used to control the disease such as chemotherapy, radiotherapy, proton beam therapy, hormone therapy, targeted drug therapy, immunotherapy etc, that causes so much suffering (Chen et al., 2020, Cammarata et al., 2020, Boing et al., 2020, Li et al., 2020).^[2] With various therapies, the surgery is also an option to remove the cancer cells from the particular organ of the body (He et al., 2020, Wahab et al., 2014).

Although numerous options are available to cure from cancer disease but the cost of the therapies or surgery is very high for the low income families. Recently, the material science and especially the nanotechnology, which is an interdisciplinary area of research and it's a best alternative for to diminish the cancer cells at a very low cost, much effective opposed to cancer cells and not to harm the body system. Towards to this direction a number of cytological studies were conducted with using nano and microstructures with different oxides and metal NPs for to retard the proliferation of cells such as cobalt oxide NPs were employed for PDTs and cytotoxic effects of materials against HepG2 cells (Iqbal et al., 2020). In other report, Bozinovic et al. describes the effect of

MoO₃NPs on human keratinocytes, with HaCaT cells via cytotoxicity, apoptosis in cells, DNA damage, ROS, and cell-survival and inflammatory signaling pathways (Božinović et al., 2020). The antimicrobial studies were conducted against S.aureus, E.coli, and P.aeruginosa by activating membrane stress in the pathogen with using molybdenum trioxide. The molybdenum trioxide (α -MoO₃) NPs were also used to study the selective cytotoxicity towards cancer cells via mitochondrial-mediated apoptotic pathway (Indrakumar et al., 2020). Including NPs, degradable nanosheets of MoO₃ structures were also utilized for the invasive cancer treatment (Qiu et al., 2021).^{[1]▶} Including to the metal oxides, a number of prominent studies were conducted with metal based nanoparticles against cancer cells such as silver NPs were used to check the in cytological change against human liver (HepG2) and **breast (MCF-7) cancer cells with** MTT, NRU assay and changes in apoptotic genes were measured by qPCR study (Khedhairi et al., 2022).^{[3]▶}

A number of utilities of nanostructures were applied for innumerable objectives whereas a very limited studies are available to show **the comparison of** oxide and metal based nanostructures for cellular cytotoxicity studies with control and gene expressions. To keep this view, **the aim of this work is to** expound **the role of** oxide (α -MoO₃NRs) and metal (AgNPs) based nanostructures against **breast cancer cells**. The structures were synthesized via solution method and characterized.^{[3]▶} The cytotoxicity's studies were showed against **breast cancer cells** (MCF-7) with using oxide and metal nanostructures. Here, the breast **cancer cell lines (MCF-7 cells) were** selected because this cancer has a major health problem worldwide. **MTT and NRU assays** were selected to check the viabilities of cancer cells (MCF-7) whereas **apoptosis in cells** caused with α -MoO₃NRs and AgNPs were investigated with the available RT-PCR study. Here, we have also explained why the NPs are much useful **to reduce the growth rate of cancer cells**.^{[3]▶}

2.0. Experimental

^[3]▶ 2.1. Material and Methods

^[7]▶ 2.1 (a) Synthesis of Molybdenum oxide nanorods (α -MoO₃NRs)

The molybdenum oxide (α -MoO₃) nanorods were conducted with the use of ammonium heptamolybdate tetra hydrate (NH₄)₆Mo₇O₂₄·4H₂O and sodium hydroxide (NaOH) via solution process as per previously published literature with minor modification (Wahab et al., 2020). In a typical experiment the (NH₄)₆Mo₇O₂₄·4H₂O (4 mM, ~0.465 g) and NaOH (0.15 M, ~0.6 g) were dissolved in double deionized distilled water (pH touches to 12.4). The solution was refluxed for 70°C for 60 min. Once the reaction was accomplished, the precipitate was kept for cooling at 25°C for ~24 h. The solution was transferred in a centrifuge tubes (~50 mL) and centrifuge at 3000 rpm for 3 min (Eppendorf, 5430R, Centrifuge, Germany) to remove the ionic impurities. Dried at room temperature in a glass petri dishes and to keep for the analysis.

2.1 (b) Synthesis of Silver Nanoparticle (AgNPs)

The AgNPs were prepared with the use of silver nitrate AgNO₃ (~0.01M) and trisodium citrate (~3 mM) in 50 mL capacity beaker as described previously with minor modification (Khedhairi et al., 2022). The reaction mixture was transferred to the black chamber, where no light enters. Keep the solution till the color changes initially brownish and then black, this change indicates the formation of AgNPs in the solution. The AgNPs was characterized well in terms of their physical and chemical characteristics.

2.1 (c) Characterizations of the prepared material

The XRD (PAN analytical XPert Pro, U.S.A.) was used to identify the crystal phases, size and crystallinity of the material with Cu_{K α} source ($\lambda = 1.54178\text{\AA}$) from 30-90° with 40kV/40mA and 6°/min angle rotation. The structured of the synthesized materials were analyzed via SEM (JSM-

6380 LA, Japan) TEM (JEOL JEM JSM 2010, Japan) as described hitherto (Wahab et al., 2014, 2020).

2.2. Cell culture (MCF-7 cells) and interaction of molybdenum oxide nanorods (α -MoO₃ NRs) and silver NPs

The cell culture was conducted with using breast cancer cells (MCF-7) grown in a medium (DMEM/MEM) including 12 % fetal bovine serum (FBS), 0.2% sodium bicarbonate, and antibiotic-antimycotic solution (100 X, 1 mL/100 mL) with humid environment (5% CO₂ & 95% O₂) at 37 °C. As per the previously reported work (Siddiqui et al., 2008)^[6], the viability of cells were evaluated by trypan blue dye and it express that more than 95% achieved viability of the cells were used in this study.^[7] Here, the cells were used between 10 to 12 passages and to treat the cells with α -MoO₃ NRs and AgNPs, used at high concentration and diluted further at desired concentrations for the exposure of cells. The cells were plated in 6-well or 96-well plates as per the experimental requirement.^[7]

2.3. Reagents and consumables

The 3-(4, 5-dimethylthiazol-2-yl)-2, 5 diphenyltetrazolium bromide which is known as MTT assay, procured from Sigma Chem.Co.USA and recycled without any alternation except dilution. Culture medium such as Dulbecco's Modified Eagle Medium (DMEM) and MEM, antibiotics-antimycotic and FBS were bought from Invitrogen, USA. The plastic wares and other consumables products for cells culture were used from Nunc, Denmark.

2.4. MTT assay

The breast cancer cells viabilities (MTT assays) with and without use of nanostructures (α -MoO₃ NRs and AgNPs) were measured as earlier protocol (Siddiqui et al., 2008, Mosmann et al., 1983).

For this, at initial the cells were sowed in 96 well plates (rate of 1×10^4 /well) with permissible to follow for 24 h at 37°C with moist environment. Here, the cells were completely exposed with nanostructures (α -MoO₃NRs and AgNPs) 1-100 μ g/mL for 24 h. Once the cells were inter mixed completely exposed in well plates, stock solution of MTT (5 mg/mL in PBS) was incorporated with rate of 10 μ L/well in 100 μ L of cell suspension and these cells were further incubated for 4 h. As the incubation was reached to their completion, the well plate's solution was with draw from the pipette and in these wells ~200 μ L of dimethyl sulfoxide (DMSO) was mixed for to aspirate the formazan product and mixed gently. Solutions optical characteristic was measured at 550 nm with micro-plate reader (Multiskan Ex, Thermo Scientific, Finland). With treated samples, the control cells were also measured as a reference and to run with same parameters. The maximum absorbance depends upon used solvent in sample solution and the level of viability of cells % was calculated as per the equations mentioned below:

$$\% \text{ viability} = [(\text{total cells-viable cells})/\text{total cells}] \times 100$$

2.5. NRU assay

Including the MTT assay, the treated (α -MoO₃NRs and AgNPs) and untreated cells (only MCF-7 cells) cytotoxic optical characteristic were also confirmed via neutral red uptake (NRU) assay as described previously (Borenfreund et al., 1985, Siddiqui et al., 2010). The MCF-7 cells (1×10^4 /well) were sowed in a specified 96 well plates. When the cells were completely grown (after 24 h), these cells were exposed with both samples at desired conc (1-50 μ g/mL) and to kept for 24 h in an incubator. After the exposure was finished, the cells were again incubated in NR medium (50 μ g/mL) for 3 h. Then the cells were completely washed and dye were removed from both samples in 1% acetic acid and 50% ethanol solution. The optical intensity of the develop color was analyzed at 540 nm.

2.6. Reactive Oxygen Species (ROS)

The ROS generation were measured with using 2, 7-dichloro dihydrofluoresce in diacetate (DCFH-DA; procured from Sigma Aldrich, USA) dye as a fluorescence agent as described method previously (Zhao et al., 2014). The cells were exposed with both nanostructures for 24 h and thereafter, cells were rinsed well with PBS and further nurtured for 30 min in DCFH-DA (20 μ M) in dark place at 37°C. The reaction of DCFH-DA dye with cells as control and treated cells were completed, and examined with using fluorescence microscope.

2.7. mRNA expressions with cancer cells (MCF-7)

The extraction of RNA was performed with cultured cells of MCF-7 cells in a 6-well plates control and treated samples at concentration of 50 μ g/mL for 24 h. For this process, the RNeasy mini Kit (Qiagen) was used to mine the RNA as per protocol instructed form manufacturer's. The cDNA was synthesized from treated and untreated cells taking 1 μ g of RNA by Reverse Transcriptase kit using MLV reverse transcriptase (GE Health Care, UK) as described protocol. The RT-PCR was completed on Roche® Light Cycler®480 (96-well block) (USA) followed with cycling program recommended. 2 μ L (40 ng) of cDNA template included the 20 μ L volume to this reaction mixture (Ahmad et al., 2020).

3.1. Result and discussion

3.1 X-ray diffraction pattern (XRD)

Fig.1 (A and B) shows the XRD of molybdenum oxide (α -MoO₃) and silver nanoparticles (AgNPs) correspondingly. From the XRD (Fig.1A), well assigned peaks were identified in XRD, which are related orthorhombic structures and analogous with the JCPDS data card no. 05-0508 and crystal lattice constants are a=3.962 Å, b=13.858 Å and c= 3.697 Å respectively. The spectrum shows a

peaks identified at defined places such as 23.21° $\langle 110 \rangle$, 25.57° $\langle 040 \rangle$, 27.14° $\langle 021 \rangle$, 29.56° (130), 33.44° $\langle 111 \rangle$, 35.29° $\langle 041 \rangle$, 38.78° $\langle 060 \rangle$, 45.99° $\langle 210 \rangle$, 49.08° $\langle 002 \rangle$, 52.59° $\langle 042 \rangle$, 54.95° $\langle 211 \rangle$ and 58.59° $\langle 112 \rangle$ respectively. The observed peaks are very similar to the crystalline α - MoO_3 , except any other impurities (Wahab et al., 2020). The estimated size of the each crystallite is ~ 50 nm, calculated with using sherrer formula. Fig.1 (B) shows the XRD pattern of AgNPs are alike to the face centered cubic (FCC) structure with metallic silver and similar to the JCPDS card no. 04-0783 with crystal lattice constant is $a=0.4086$ nm correspondingly. The spectrum illustrates the indexed and assign peaks with their related positions such as 38.17° $\langle 111 \rangle$, 44.29° $\langle 200 \rangle$, 64.40° $\langle 220 \rangle$, 77.37° $\langle 311 \rangle$ and 81.49° $\langle 222 \rangle$ respectively, with an individual crystallite size was ~ 15 nm (Khedhairi et al., 2022).

3.2. Morphological studies of α - MoO_3 NRs and AgNPs

3.2. (a) SEM and TEM results

The structural detail of the products were examination with SEM images captured at low and high magnification scale and presented as Fig.2. At low magnified scale image (Fig.2A) of α - MoO_3 NRs shows the formation of several rod shaped structures that are arranged in manner as composed to form circular spheres shaped structure. The image was further identified at high scale which show the individual structure (Fig.2B). It observed from the images that the average diameter of an individual NRs is in range of ~ 50 - 60 nm, whereas length exceeds to 1 - 2 μm (Fig.2B). In other images captured at low (Fig.2C) and high (Fig.2D) scale magnification shows several AgNPs are arranged on the whole surfaces. The average size of each NP is ~ 15 nm, which smooth surface morphology.

Further for more clarification, the samples were also analyzed with TEM and represent as Fig.3A. A number of several rods shaped structure of α - MoO_3 are appeared on surfaces with an average

diameter is ~50-60 nm and 1-2 μm length respectively. In other image shows a number of small particles with nanometer scale is seen with an individual size is ~15 nm (Fig.3B). The obtained images authenticated that the NPs surfaces are smooth, clear and are fully consistent with SEM analysis (Fig.2).

3.3 General cancer cells (MCF-7) morphology and their change with used nanostructures

The cells were cultured as described above protocol and the morphological study was observed via microscopy at 24 h incubation periods at 100 $\mu\text{g}/\text{mL}$ of nanostructures (Fig.4). The captured image of MCF-7 cancer cells (Fig.4A-Control) whereas others images were captured with treated samples at 100 $\mu\text{g}/\text{mL}$ concentration of $\alpha\text{-MoO}_3$ (Fig.4B) and AgNPs (Fig. 4C) respectively. From the observed images, it represents that the cells were nucleated and once their confluences reached to their enhanced confluence (~70-80 %,) treated with nanostructures ($\alpha\text{-MoO}_3\text{NRs}$ and AgNPs) and analyzed. The observation reveals that there is no noteworthy change was noticed at an initial range of concentration of the nanostructures (1, 2, 5, 10 and 25 $\mu\text{g}/\text{mL}$ data not shown), but once the concentration of $\alpha\text{-MoO}_3$ and AgNPs upsurges to 50 to 100 $\mu\text{g}/\text{mL}$, the growth of the cells were much affected. The microscopic images authenticated that the cells were damaged with the incorporation of $\alpha\text{-MoO}_3\text{NRs}$ and AgNPs.

3.4. The induced cytotoxicity (MTT assay) with processed $\alpha\text{-MoO}_3\text{NRs}$ and AgNPs

As described in the material and method section that the untreated (control) breast cancer cells (MCF-7) and treated cells (MCF-7 cells with nanostructures) samples were exposed in a range of different concentrations from 1-100 $\mu\text{g}/\text{mL}$ for 24 h incubation. The cytotoxicity's were examined through MTT assay. The obtained optical densities data shows viability of cancer cells were diminished with the incorporation of $\alpha\text{-MoO}_3\text{NRs}$ and AgNPs and these data's were concentration/

dose-dependent.^{[1]▶} In case of α -MoO₃NRs, the MCF-7 cells viability, MTT assay was decreases at 24 h 101%, 102%, 102%, 103%, 89%, 79% and 63% (Fig.5A)^{[2]▶} for the conc of 1, 2, 5, 10, 25, 50 and 100 μ g/mL correspondingly (p 0.05 for each). In case of AgNPs, the MCF-7 cells viability, MTT assay was decreases at 24 h 101%, 101%, 98%, 94%, 62%, 54% and 49% (Fig.5B) for the conc of 1, 2, 5, 10, 25, 50 and 100 μ g/mL correspondingly (p 0.05 for each). The recovered data's shows that cells viabilities were not much affected at initial concentration, whereas when the conc/doses of α -MoO₃NRs and AgNPs were exceeded to their optimum level, the cytotoxicity's were much influenced (Siddiqui et al., 2008).

3.5. Cytotoxicity study via NRU assay in MCF-7 cells with different nanostructures

Apart from the MTT assay, the cytotoxic measurements were also verified non-treated and treated nanostructures via NRU assays as detailed in the materials and method. A similar observation were also found in NRU assays.^{[2]▶} As described in the MTT section, the NRU data also in consistent and shows that that the viabilities of cancer cells at initial conc of nanostructures (α -MoO₃NRs and AgNPs) were not much influenced, whereas once the conc increases, the growth of cancer cells were reduced.^{[1]▶} In case of α -MoO₃NRs, for the MCF-7 cells, NRU assay was decreases at 24 h 102%, 101%, 104%, 100%, 91%, 84% and 60% (Fig.6A) for the conc of 1, 2, 5, 10, 25, 50 and 100 μ g/mL correspondingly (p 0.05 for each).^{[1]▶} In case of AgNPs, for MCF-7 cells, NRU assay was decreases at 24 h 98%, 97%, 93%, 90%, 69%, 64% and 51% (Fig.6B) for the conc of 1, 2, 5, 10, 25, 50 and 100 μ g/mL correspondingly (p 0.05 for each) (Siddiqui et al., 2010).

3.6. Induced ROS generation in MCF-7 with nanostructures^{[9]▶}

A similar and sequential trends were also observed in ROS generations detected in MCF-7 cells after the exposure of α -MoO₃ and AgNPs at 25 to 100 μ g/mL concentrations for 24 h (Fig.7). The

ROS is increases with AgNPs and it's evident from the image (Fig.7A) as compared to control cells. An increase of 108%, 125% and 160% of ROS generation were observed with the interaction of α -MoO₃ in MCF-7 Cells at 25, 50 and 100 μ g/mL, as compared to control (Fig.7B). The ROS formed more 118%, 135% and 177% with the interaction of AgNPs at 25, 50 and 100 μ g/mL conc. in MCF-7 cells as compared to control in 24 h (Zhao et al., 2014).

3.7. Gene expressions study

The real time PCR was utilized for to understand the mRNA levels of apoptotic and anti-apoptotic marker genes (e.g. p53, Bax, caspase-3, caspase-3 and BCL₂) in MCF-7 cells interacted with both α -MoO₃NRs and AgNPs at 50 μ g/mL for 24 h. A noteworthy changes were observed in mRNA levels in apoptotic markers (p53, Bax, caspase-3, caspase-9 and BCL₂) genes in MCF-7 cells, once exposed with α -MoO₃NRs and AgNPs (Fig.8). The mRNA tumor suppression gene supports the apoptosis induction by α -MoO₃NRs and observed the enzymatic activities of caspase-3 at the conc of 50 μ g/mL. The obtained results of mRNA gene expression with all chosen gene were in down-regulation and the fold changes for the p53 (2.7), Bax (3.3), Casp3 (2.3), Casp9 (2.6) and BCL₂ (0.71) in α -MoO₃NRs whereas in case of AgNPs the gene expression fold changes are p53 (3.9), Bax (4.1), Casp3 (2.7), Casp9 (2.9) and BCL₂ (0.85) respectively. A detailed investigation is required to testify the nanostructures as well as the results represent that NPs induced the apoptotic enzymes (casp3, Casp9) in a dose-dependent manner (Ahmad et al., 2022).

4. Conclusions

The summary of the present work displayed that the α -MoO₃ nanorods (diameter ~50-60 nm, length 1-2 μ m) and AgNPs (size ~15 nm) were synthesized via solution process and were characterized. The α -MoO₃ nanorods and AgNPs were used at low to high concentrations range (1 to 100

$\mu\text{g/mL}$) against MCF-7 cancer cells, which indicates that the cytotoxicity of MCF-7 cells influence against cancer cells and are dose reliant validated via MTT and NRU assays. The cells in apoptosis were happened with the NPs at optimized doses of conc (50 $\mu\text{g/mL}$).^[21] The present work infers that the as compared to the $\alpha\text{-MoO}_3$ rods, AgNPs have more possibilities and high reactivity against breast cancer cells. These metal based NPs are much effective as compared to available organic compounds and their sustainability required under biological conditions. The study typify that NPs induces the cytotoxicity, apoptosis in MCF-7 cancer cells via p53, Bax, and caspase pathways, whereas Bcl2 act as an anti-apoptotic marker gene for cancer cells and are consistent with other data's.^[2] The ROS generation increased in cancer cells, due to the interaction of $\alpha\text{-MoO}_3$ rods and AgNPs.^[2] From the entire experiment and their results it suggest that NPs are much effective and are responsible to regulate the growth of cancer cells.^[2] Due to the unique size and small diameter facilitates NPs and it can be easily entered in to the cells organelles and reacted fast against cancer cells.^[2] The utility of these NPs against cancer studies may possible to reduce the cost of the preparation of drugs also studies reduces the anxiety of surgery for the deprived patient.

Acknowledgement:^[10] The authors extend their appreciation to the Deputyship for Research & Innovation, Ministry of Education in Saudi Arabia for funding this research (IFKSURC-1-3207).^[22]

Conflict of interest statement:^[8] The authors declare that they have no known competing financial interests.

Figure Captions

Fig.1. shows the XRD pattern of α -MoO₃ (A) and AgNPs (B) respectively. Whereas*shows the unidentified peaks in the spectrum.

Fig.2. ^[27] SEM images of α -MoO₃: (A captured at 3000x and B at 27,000x) magnification whereas (C captured at 30000x and D at 60,000x) shows the AgNPs size. The estimated size of an individual NR diameter is ~50 nm and length is ~1-2 μ m whereas individual NP size is ~15 nm respectively.

Fig.3. TEM displayed the images of α -MoO₃NRs (A captured at 1000x) and AgNPs (B captured at 50000x) respectively.

Fig.4. The morphology of the MCF-7 (control A) and their structural change exposed with α -MoO₃NRs (B) and AgNPs (C) for 24 h. Images were captured under the phase contrast inverted microscope.

Fig.5. The study of cytotoxicity via MTT assay in MCF-7 cells succeeding the exposure of α -MoO₃NRs (A) and AgNPs (B) for 24 h. The experiments were conducted in triplicate manner (Mean \pm SD triplicate).

Fig.6. The study of cytotoxicity via NRU assay in MCF-7 cells succeeding the exposure of α -MoO₃NRs (A) and AgNPs (B) for 24 h. The experiments were conducted in triplicate manner (Mean \pm SD triplicate).

Fig.7 (A) Representative images of α -MoO₃NRs and AgNPs induced ROS in MCF-7 cells exposed for 24 h. (B) Percent change in ROS with MCF-7 at varied conc of α -MoO₃NRs and AgNPs respectively.

Fig.8. mRNA expression of apoptosis marker genes by RT-PCR analysis in MCF-7 cells with α -MoO₃NRs and AgNPs at 50 μ g/mL concentration for 24 h. RT-PCR data was achieved with Roche Light Cycler@480 soft-ware (version 1.5). The glyceraldehyde 3-phosphate dehydrogenase (GAPDH) gene was used as a control to normalize data. ^[11] The data is accessible as the mean \pm SD of three identical experiments with three replicates manner. ^[3] *Significantly different associated with the control group (p 0.05 for each).